BIOCHEMICAL PHARMACOLOGY 74 (2007) 1253–1262

available at www.sciencedirect.com

ScienceDirect

journal homepage: www.elsevier.com/locate/biochempharm

A-366833: A novel nicotinonitrile-substituted 3,6-diazabicyclo[3.2.0]-heptane α4β2 nicotinic acetylcholine receptor selective agonist: Synthesis, analgesic efficacy and tolerability profile in animal models

Jianguo Ji [a,*], *William H. Bunnelle* [a,*], *David J. Anderson* [a], *Connie Faltynek* [a], *Tino Dyhring* [b], *Philip K. Ahring* [b], *Lynne E. Rueter* [a], *Peter Curzon* [a], *Michael J. Buckley* [a], *Kennan C. Marsh* [a], *Anita Kempf-Grote* [a], *Michael D. Meyer* [a]

[a] *Neuroscience Research, Department-R47W, Bldg.-AP9A, Global Pharmaceutical Research and Development, Abbott, Abbott Park, IL 60064, USA*

[b] *NeuroSearch A/S, Ballerup, Denmark*

ARTICLE INFO

Article history:
Received 4 June 2007
Accepted 8 August 2007

Keywords:
nAChR
Nicotine
Epibatidine
A-366833
Pain
Emesis

ABSTRACT

5-[(1R,5S)-3,6-Diazabicyclo[3.2.0]heptan-6-yl]nicotinonitrile (A-366833) is a novel nicotinic acetylcholine receptor (nAChR) ligand that binds to the agonist-binding site ([^{3}H]-cytisine) with K_i value of 3.1 nM and exhibits agonist selectivity at α4β2 nAChR relative to the α3β4 nAChR subtype. The analgesic effects of A-366833 were examined across a variety of animal models including the mouse model of writhing pain (abdominal constriction), the rat models of acute thermal (hot box), persistent chemical (formalin) and neuropathic (spinal nerve ligation, SNL) pain. In the abdominal constriction model, A-366833 was effective at doses ranging from 0.062 to 0.62 μmol/kg (i.p.). In addition, A-366833 demonstrated significant effects in acute thermal pain (6.2–19.0 μmol/kg, i.p.), formalin (1.9–19 μmol/kg i.p.) and SNL (1.9–19 μmol/kg i.p.) models. The systemic effects of A-366833 were attenuated by pretreatment with mecamylamine (5 μmol/kg i.p.) in both the formalin and SNL models, suggesting that the analgesic effects of A-366833 in models of persistent nociceptive and neuropathic pain are mediated by activation of nAChRs. Pharmacokinetic investigations of A-366833 in rat revealed moderate brain:plasma distribution, half-life of 1.5 h and excellent oral bioavailability of 73%. Comparison of peak plasma levels at the minimal effective doses across rat models of acute thermal pain, formalin and SNL with the maximal exposure that does not evoke emesis in ferret revealed therapeutic margins ranging from 6- to 22-fold. These studies indicate that compounds like A-366833 with improved agonist selectivity at α4β2 vs. α3β4 nAChR can elicit a broad spectrum of analgesic efficacy without concurrent adverse effects.

* *Corresponding authors*. Tel.: +1 847 935 3579/1 847 938 9765; fax: +1 847 937 9195.
E-mail addresses: jianguo.ji@abbott.com (J. Ji), william.h.bunnelle@abbott.com (W.H. Bunnelle).

0006-2952/$ – see front matter
doi:10.1016/j.bcp.2007.08.010

1. Introduction

Among numerous approaches aimed at satisfying the significant unmet medical need for the management of severe pain [1], those targeting nicotinic acetylcholine receptors (nAChR) with ligands that exhibit superior efficacy and tolerability profiles continue to receive considerable attention [2–4]. It is well recognized that nicotine (**1**), as well other nAChR agonists including epibatidine (**2**), demonstrate significant antinociceptive effects across a variety of rodent pain models [5–8]. Clinical validation of the nAChR approach has been achieved, but development of first generation nAChR agents for the management of moderate-to-severe pain has been limited due to adverse effects such as emesis and nausea [9–13]. The search for second-generation nAChR analgesics has been driven by the hypothesis that side effects are attributable to poor selectivity among nAChR subtypes [14]. nAChRs are pentameric ligand-gated ion channel proteins that are widely expressed throughout the central and peripheral nervous systems including in regions associated with nociceptive transmission. Neuronal nAChRs are derived from multiple α (α2–α10) and β (β2–β4) subunit genes. Each distinct subunit gene composition defines a certain nAChR subtype, with characteristic pharmacological and biophysical properties [15]. While the nAChR subunit combinations that mediate analgesic effects remain to be precisely defined, two distinct mechanisms for nAChR-mediated effects have been identified. The first, which requires receptor activation by agonists, can involve peripheral and central sites of action and appears to be responsible for the analgesic properties of compounds like epibatidine and A-85380 [6,16]. A growing body of evidence, largely from gene knockout and antisense studies, strongly implicates the involvement of the α4β2 nAChR combination in this type of nAChR agonist mediated antinociception [17–21]. On the other hand, the α3β4 nAChR combination predominates in the sympathetic ganglia and is thought to mediate adverse events such as gastrointestinal effects [14]. Accordingly, medicinal chemistry efforts over the past few years have primarily focused on the identification of selective α4β2 nAChR agonists to test the hypothesis that robust analgesic efficacy with wider tolerability vs. adverse effects can be achieved [2–8]. More recently, blockade of α9α10 nAChRs has also been shown to alleviate chronic pain resulting from peripheral nerve injury or inflammation, possibly via neuro-immunomodulatory mechanims [22–24].

Our in-house efforts to discover second generation α4β2 nAChR subtype selective agonists with diminished interactions at the α3β4 nAChRs, led to the discovery of novel nicotinonitrile-substituted 3,6-diazabicyclo[3.2.0]heptane nAChR ligands represented by compounds including A-366833 (**3**), A-365193 (**4**), A-424600 (**5**) and A-369452 (**6**) Fig. 1 [25]. This study describes the chiral synthesis, binding and functional evaluation of compounds **3–6**. Among the analogs evaluated, 5-[(1R,5S)-3,6-diazabicyclo[3.2.0]heptan-6-yl]nicotinonitrile (A-366833, **3**) emerged as an α4β2 nAChR subtype selective agonist, and accordingly, was further characterized in vivo across models of efficacy and tolerability.

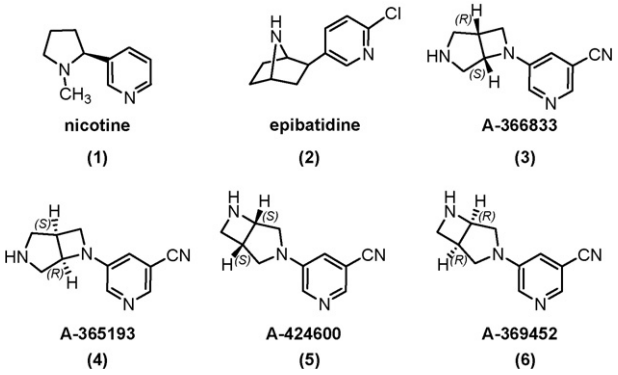

Fig. 1 – Chemical structures of nicotine, epibatidine and 3,6-diazabicyclo[3.2.0]heptane nAChR agonists used in this study.

2. Materials and methods

2.1. Compound synthesis

2.1.1. A-366833, 5-[(1R,5S)-3,6-diazabicyclo[3.2.0]heptan-6-yl]nicotinonitrile (3)

Under N_2, (1S,5S)-benzyl 3,6-diazabicyclo[3.2.0]heptane-3-carboxylate [25] (4.64 g, 20.0 mmol) was stirred with 5-bromonicotinonitrile (5.50 g, 30.0 mmol), $Pd_2(dba)_3$ (366 mg, 0.4 mmol), BINAP (0.75 g, 1.2 mmol) and Cs_2CO_3 (13.12 g, 40.0 mmol) in anhydrous toluene (200 mL) at 110 °C for 40 h. The reaction mixture was cooled to ambient temperature and the solid was removed by filtration. The organic filtrate was concentrated under reduced pressure, and the residue was purified by chromatography (SiO_2, eluted with EtOAc/hexane = 80/20, R_f = 0.30) to give (1S,5S)-benzyl 6-(5-cyanopyridin-3-yl)-3,6-diazabicyclo[3.2.0]heptane-3-carboxylate (6.1 g, 91.3% yield) as white solid: mp 101.4–102.9 °C; $[\alpha]_D^{20} = -277.46°$ (c = 0.43, MeOH)]. This was taken in trifluoroacetic acid (30.0 mL) and stirred at 65 °C. After 1 h, the mixture was concentrated under reduced pressure. The residue was basified to pH = 8–9 with 1N NaOH and extracted with $CHCl_3$ (3 × 50 mL). The combined extract was concentrated to an oil that was purified by chromatography (SiO_2, eluted with CH_2Cl_2/MeOH/$NH_3{\cdot}H_2O$ = 90/10/2, R_f = 0.15) to provide A-366833 as the free base (mp: 101.4–102.9 °C). This material (1.40 g, 7 mmol) was converted to bis(tosylate) salt by stirring with *p*-TsOH·H_2O (2.66 g, 14.0 mmol) in ^{i}PrOH (50 mL) at 80 °C for 1 h, then at ambient temperature for 10 h. The salt was crystallized, collected by filtration and dried under vacuum (3.20 g, 84.0% yield). mp 240–243 °C; ^{1}H NMR (MeOH-D_4, 400 MHz) δ 2.36 (s, 6H), 3.23 (dd, J = 13.0, 3.8 Hz, 1H), 3.34 (dd, J = 12.6, 7.1 Hz, 1H), 3.73 (d, J = 12.3 Hz, 1H), 3.82–3.98 (m, 3H), 4.18 (t, J = 8.6 Hz, 1H), 5.13 (dd, J = 6.4, 3.7 Hz, 1H), 7.21 (d, J = 8.0 Hz, 4H), 7.64 (d, J = 8.0 Hz, 4H), 7.83 (dd, J = 2.6, 1.4 Hz, 1H), 8.22 (d, J = 2.5 Hz, 1H), 8.42 (d, J = 0.9 Hz, 1H) ppm; MS (DCI/NH_3) m/z 218 $(M + NH_4)^+$, 201 $(M + H)^+$. Anal. Calcd. for $C_{11}H_{12}N_4{\cdot}2.00C_7H_8SO_3$: C, 55.13; H, 5.18; N, 10.29. Found: C, 55.04; H, 4.93; N, 9.96.

2.1.2. A-365193, 5-[(1S,5R)-3,6-diazabicyclo[3.2.0]heptan-6-yl]nicotinonitrile (4)

The free base of A-365193 was prepared according to the procedure described for A-366833, with the exception that

(1*R*,5*R*)-benzyl 3,6-diazabicyclo[3.2.0]heptane-3-carboxylate [25] was used as the starting material. The free base was converted to the bis(fumarate) salt by stirring with two equivalents of fumaric acid in EtOAc/EtOH (10/1) for 10 h. The salt was crystallized, collected by filtration and dried under vacuum. ^{1}H NMR (MeOH-D_4, 400 MHz) δ 3.20 (dd, J = 12.7, 3.7 Hz, 1H), 3.35–3.42 (m, 1H), 3.48–3.53 (m, 1H), 3.70–3.85 (m, 3H), 4.10 (t, J = 8.1 Hz, 1H), 5.00 (dd, J = 6.5, 3.8 Hz, 1H), 6.70 (s, 5.0H), 7.36 (d, J = 2.7, 1.7 Hz, 1H), 8.10 (d, J = 3.0 Hz, 1H), 8.26 (d, J = 1.4 Hz, 1H) ppm; MS (DCI/NH_3) m/z 218 $(M + NH_4)^+$, 201 $(M + H)^+$. Anal. Calcd. for $C_{11}H_{12}N_4{\cdot}2.50C_4H_4O_4{\cdot}0.70H_2O$: C, 50.14; H, 4.69; N, 11.14. Found: C, 49.83; H, 4.30; N, 11.10.

2.1.3. A-424600, 5-[(1*S*,5*S*)-3,6-diazabicyclo[3.2.0]heptan-3-yl]nicotinonitrile (5)

The free base of A-424600 was prepared from (1*R*,5*S*)-*tert*-butyl 3,6-diazabicyclo[3.2.0]heptane-6-carboxylate [25] according to the procedure described for A-366833 and then converted to the tosylate salt by stirring with 1.2 equivalents of *p*-TsOH·H_2O in EtOAc/EtOH (10/1) for 10 h. The salt was crystallized, collected by filtration and dried ^{1}H NMR (MeOH-D_4, 300 MHz) δ 2.30 (s, 4.2H), 3.16 (dd, J = 10.7, 6.3 Hz, 1H), 3.25 (dd, J = 12.8, 7.8 Hz, 1H), 3.47–3.62 (m, 1H), 3.74 (dd, J = 11.2, 5.1 Hz, 1H), 3.98 (d, J = 10.5 Hz, 1H), 4.20 (d, J = 12.5 Hz, 1H), 4.28 (dd, J = 11.0, 8.6 Hz, 1H), 5.08 (dd, J = 6.8, 5.1 Hz, 1H), 7.22 (d, J = 8.1 Hz, 2.8H), 7.69 (d, J = 8.5 Hz, 2.8H), 7.76 (dd, J = 2.7, 1.7 Hz, 1H), 8.39 (d, J = 1.7 Hz, 1H), 8.47 (d, J = 2.7 Hz, 1H) ppm; MS (DCI/NH_3) m/z 201 $(M + H)^+$; Anal. Calc. for $C_{11}H_{12}N_4{\cdot}1.40C_7H_8SO_3$: C, 56.61; H, 5.30; N, 12.70. Found: C, 56.74; H, 5.29; N, 12.49.

2.1.4. A-369452, 5-[(1*R*,5*R*)-3,6-diazabicyclo[3.2.0]heptan-3-yl]nicotinonitrile (6)

The free base of A-369452 was prepared from (1*S*,5*R*)-*tert*-butyl 3,6-diazabicyclo[3.2.0]heptane-6-carboxylate [25] according to the procedure described for A-366833 and then converted to the fumarate salt by stirring with 1.2 equivalents of fumaric acid in EtOAc/EtOH (v. 10/1) for 10 h. The salt was crystallized, collected by filtration and dried under vacuum. ^{1}H NMR (MeOH-D_4, 300 MHz) δ 3.14 (dd, J = 10.6, 6.2 Hz, 1H), 3.24 (dd, J = 12.8, 5.0 Hz, 1H), 3.55 (m, 1H), 3.75 (dd, J = 11.0, 5.0 Hz, 1H), 3.96 (d, J = 10.6 Hz, 1H), 4.18 (d, J = 12.2 Hz, 1H), 4.28 (dd, J = 10.9, 8.4 Hz, 1H), 5.00 (dd, J = 6.8, 4.8 Hz, 1H), 6.40 (s, 2H), 7.65 (dd, J = 2.9, 1.2 Hz, 1H), 8.33 (d, J = 1.2 hz, 1H), 8.45 (d, J = 2.8 Hz, 1H) ppm; MS (DCI/NH_3) m/z 201 $(M + H)^+$; Anal. Calc. for $C_{11}H_{12}N_4{\cdot}1.00C_4H_4O_4{\cdot}0.50H_2O$: C, 55.38; H, 5.27; N, 17.22. Found: C, 55.00; H, 5.27; N, 17.06.

2.2. *In vitro assays*

2.2.1. [^{3}H]-Cytisine binding

[^{3}H]-Cytisine binding assay conditions were modified from the procedures described in Pabreza et al. [26]. Membrane enriched fractions from rat brain minus cerebellum (ABS Inc., Wilmington, DE) were slowly thawed at 4 °C, washed and resuspended in 30 vol of BSS–Tris buffer (120 mM NaCl; 5 mM KCl; 2 mM $CaCl_2$; 2 mM $MgCl_2$; 50 mM Tris–Cl, pH 7.4, 4 °C). Samples containing 100–200 μg of protein and 0.75 nM [^{3}H]-cytisine (30 C_i/mmol; Perkin Elmer/NEN Life Science Products, Boston, MA) were incubated in a final volume of 500 μL for 75 min at 4 °C. Seven log-dilution concentrations of each compound were tested in duplicate. Non-specific binding was determined in the presence of 10 μM of (−)-nicotine. Bound radioactivity was isolated by vacuum filtration onto pre-wetted glass fiber filter plates (Millipore, Bedford, MA) using a 96-well filtration apparatus (Packard Instruments, Meriden, CT) and were then rapidly rinsed with 2 mL of ice-cold BSS buffer (120 mM NaCl/5 mM KCl/2 mM $CaCl_2$/2 mM $MgCl_2$). Packard MicroScint-20® scintillation cocktail (40 μL) was added to each well and radioactivity determined using a Packard TopCount® instrument.

2.2.2. Fluorometric imaging plate reader (FLIPR)-based functional assay

HEK-293 cell lines expressing the recombinant human nAChRs (α4β2 and α3β4 subunit combinations) were used in the determination of functional nAChR agonist activity by measuring intracellular calcium changes using the fluorometric imaging plate reader (FLIPR; Molecular Devices, Sunnyvale, CA, USA). Cells were plated at densities of 25,000–50,000 cells/well in DMEM (GIBCO) supplemented with 10% FBS (GIBCO) in 96-well clear bottom black walled plates precoated with poly-D-lysine (Sigma, 75 μL/well of 0.01 g/L solution ≥30 min) and allowed to incubate for 24–48 h at 37 °C in 5% CO_2 in a humidified environment. After aspirating off the media, the cell lines were incubated in the dark at room temperature for 45–60 min with 2–4 μM Fluo-4 AM calcium indicator dye (Molecular Probes, Eugene, OR) dissolved in 0.1 to 0.2% (v/v) of DMSO (Sigma, UK) in NMDG Ringer buffer (in mM: 140 NMDG, 5 KCl, 1 $MgCl_2$, 10 HEPES, 10 $CaCl_2$, pH = 7.4). Cells were placed in the FLIPR and 50 μL of 3× stock concentrations of test compounds or buffer prepared in the same NMDG ringer buffer were added. Raw fluorescence data were corrected by subtracting fluorescence values from wells that received buffer only additions. Peak fluorescent values were exported to Microsoft Excel, corrected for background signal and expressed as a percentage of the reference peak response for the positive control of 100 μM nicotine.

2.3. *In vivo studies*

2.3.1. Animals

Adult male mice (Jackson Laboratories, Bar Harbor, ME), Sprague–Dawley rats (Charles River, Portage, MI) and male ferrets (Marshall BioResources, North Rose, NY) were used for the studies. These animals were housed in AAALAC-approved facilities at Abbott Laboratories in a temperature-regulated environment with lights on between 7:00 a.m. and 10:00 p.m. Food and water were available *ad libitum* at all times except during testing. Studies were conducted following procedures outlined in protocols approved by Abbott's Institutional Animal Care and Use Committee.

2.3.2. Abdominal construction model

Experiments were performed using mice weighing 20–25 g (Jackson Laboratories, Bar Harbor, ME) as described previously [27]. A solution of A-366833 bis(tosylate) was prepared in saline and injected (i.p.). After 30 min 0.3 mL of 0.6% acetic acid was dosed (i.p.) to evoke writhing. Animals were placed separately under clear cylinders for observation and quantification of abdominal constriction responses. These responses were

defined as a mild constriction and elongation passing caudally along the abdominal wall, accompanied by a slight twisting of the trunk and followed by bilateral extension of the hind limbs. The total number of abdominal constrictions was recorded from 5 to 20 min after the acetic acid injection. Results are presented as percent of responses relative to vehicle-treated animals.

2.3.3. *Acute thermal pain model (hot box)*

For hot-box experiments, a commercially available paw thermal stimulator was used as previously described [8]. Rats were placed in Plexiglas cubicles that were located on a glass surface of the apparatus. The surface of the glass was maintained at 30 °C. A thermal stimulus was applied to the bottom of the rear foot of the rat *via* a movable focused projection bulb. The stimulus current was maintained at 4.8 amp. The latency until the animal moved its foot from the stimulus was recorded automatically by use of photodiode motion sensors. A 20-s cut-off was used to limit possible tissue damage after exposure to the stimulus. For any given measure (*e.g.*, time point), one foot of each of the six animals was tested and then the process was repeated for the opposite foot. All studies began with a 20-min acclimation period. After determination of base line responses, compound was administered (i.p.) and measures were taken 15, 30 and 45 min post-treatment.

2.3.4. *Formalin model*

Male Sprague–Dawley rats weighing 200–400 g were used in all experiments as previously described [28]. Injection of formalin (50 μL of 5% formalin in saline) into the dorsal aspect of the rat rear paw produces a transient inflammatory response (Phase 1) [29], and characterized by behaviors including licking, biting and flinching the affected paw. This acute phase subsides after about 10 min, with the nocifensive behavior renewed (about 20 min post-dose) in a persistent response (Phase 2) that is considered to reflect central sensitization. In this study, only the Phase 2 response was scored. A-366833 was dosed (i.p.) 5 min prior to administration (s.c.) of formalin (50 μL of 5% formalin in saline) into the dorsal aspect of one of the rear paws. Animals were then returned to the clear observation cages suspended above mirror panels. Effects of A-366833 were evaluated in the time interval 30–50 min after the administration of formalin (Phase 2 response). The number of flinches was recorded as a measure of persistent pain for 6–8 rats per dose group. In experiments designed to assess the role of nAChRs, mecamylamine was administered 10 min before A-366833 treatment.

2.3.5. *Spinal nerve (L5-L6) ligation model*

Male Sprague–Dawley rats weighing 80–100 g at the time of surgery were used for all experiments. Prior to surgery, animals were group-housed and maintained in a temperature-regulated environment as described above. Under halothane anesthesia, the L5 and L6 spinal nerves were tightly ligated in the manner described previously by Chung et al. [30]. An incision was made on the dorsal portion of the hip and the muscle was blunt dissected to reveal the spinal processes. The L6 transverse process was removed, and the left L5 and L6 spinal nerves were tightly ligated with 5.0-braided silk suture. The wound was cleaned, the membrane sewn with 4.0 dissolvable Vicryl suture and the skin closed with wound clips. Following nerve ligation surgery, animals were group-housed. Rats had access to food and water ad libitum. Two weeks after surgery, rats were acclimated to the testing box that was constructed of Plexiglas with a wire mesh floor to allow access to the planter surface of the hind paws. On the testing days, mechanical allodynia in the affected paw of animals that had undergone spinal nerve ligation was evaluated using von Frey filaments. The maximal withdrawal threshold was 15 g. Using the Dixons up–down method, the baseline level of allodynia was determined, with allodynia defined as a withdrawal threshold $\leq$4 g of pressure. Immediately after baseline testing, a saline solution of A-366833 was administered intraperitoneally, and subsequent withdrawal thresholds were determined 15, 30, 60 and 120 min post-dosing. In experiments designed to assess the role of nAChRs, mecamylamine was administered (i.p.) after baseline testing, 10 min prior to the administration of A-366833.

2.3.6. *Emetic effects in ferrets*

Male ferrets weighing 1–1.7 kg were used in all experiments as described previously [31,32]. Animals were fasted overnight before emesis testing. Briefly, animals were placed in individual polycarbonate cages with ventilated tops and allowed to acclimate to the experimental room for 1 h prior to commencing study. A-366833 was dissolved in vehicle (saline) and administered (i.p.). After dosing, the animals were observed for emetic responses for a period of 90 min. The percentage of animals that experienced emesis was recorded.

2.3.7. *Data analysis*

In radioligand binding experiments, the IC_{50} values were determined by nonlinear regression using Microsoft Excel® software and K_i values were calculated using the Cheng-Prusoff equation, where $K_i = IC_{50}/(1 + [\text{ligand}]/K_D)$. For calcium flux experiments, concentration-response data were fitted using a single sigmoidal function in GraphPad Prism (San Diego, CA) for determination of EC_{50} and maximum response values. Statistical analysis was performed using either *t*-test or one-way ANOVA. $P < 0.05$ was considered significant. Data are expressed as means ± S.E.M.

3. Results

3.1. *In vitro pharmacology*

The predominant receptor with high affinity to (−)-[^{3}H]-cytisine binding in rodent brain is composed of α4 and β2 subunits [33,34]. The binding affinities of ligands at nAChRs were determined by assessing their ability to displace (−)-[^{3}H]-cytisine binding to rat brain membranes [35]. The K_i values of the compounds for displacing rat brain [^{3}H]-cytisine binding is shown in Table 1, A-366833 (**3**) shows binding affinity (K_i = 3.1 nM), comparable to that of nicotine (**1**) (K_i = 1.0 nM), but substantially less potent than epibatidine (**2**) (K_i = 0.05 nM). The affinities for A-365193 (**4**) and A-424600 (**5**) are slightly higher. A-369452 (**6**) demonstrated the highest binding affinity (K_i = 0.1 nM) among four isomers **3–6** tested.

Table 1 – Comparative in vitro properties of nicotinonitrile-substituted 3,6-diazabicyclo[3.2.0]-heptanes (3–6) and nicotine (1), as well epibatidine (2) in radioligand binding and functional assays

Compounds	[^{3}H]-cyt.[a]	Ca^{2+} flux (FLIPR)			
	K_i (nM) (pK_i)	hα4β2		hα3β4	
		EC_{50}[b] (μM) (pEC_{50})	Max. (%)[c]	EC_{50}[b] (μM) (pEC_{50})	Max. (%)[c]
A-366833	3.1 (8.50 ± 0.17)	5.9 (5.29 ± 0.10)	65 ± 2	N.C.[d]	16 ± 2
A-365193	0.9 (9.07 ± 0.05)	11.4 (5.04 ± 0.34)	34 ± 2	13.7 (4.91 ± 0.15)	47 ± 8
A-424600	1.7 (8.77 ± 0.06)	14.6 (4.88 ± 0.08)	102 ± 6	7.1 (5.15 ± 0.03)	84 ± 3
A-369452	0.1 (9.92 ± 0.05)	0.6 (6.38 ± 0.17)	123 ± 5	0.3 (6.49 ± 0.02)	102 ± 3
Nicotine	1.0 (9.03 ± 0.31)	6.6 (5.18 ± 0.06)	101 ± 3	8.0 (5.10 ± 0.04)	89 ± 3
Epibatidine	0.05 (10.33 ± 0.13)	0.05 (7.27 ± 0.04)	133 ± 13	0.01 (7.92 ± 0.07)	103 ± 15

[a] Displacement studies with [^{3}H]-cytisine using rat brain membranes. The K_i represents mean values obtained from at least three independent experiments.
[b] Values represent mean potencies of compounds, assessed by measuring fluorescence changes using FLIPR technology in HEK 293 cell lines expressing human α4β2 and α3β4 nAChRs.
[c] Max. values represent maximal response of the ligand relative to the peak response for the positive control of 100 μM nicotine.
[d] NC, EC_{50} not reliably calculable for agonists with maximal response below 20%.

In calcium flux assays, functional interactions were assessed at hα4β2 and hα3β4 nAChRs [36,37]. At the recombinant human α4β2 nAChR subtype, A-366833 exhibited a potency (EC_{50} = 5.9 μM) similar to nicotine, but A-366833 is somewhat less efficacious with a maximal response 65% relative to nicotine. At the α3β4 subtype, A-366833 is much less active than nicotine, exhibiting only about 16% efficacy at the highest concentration tested (100 μM, Table 1). Thus, A-366833 is a moderately potent partial agonist at the α4β2 nAChR, with little or no agonist activity at the α3β4 subtype. In comparison, epibatidine **2** is approximately 100–150-fold more potent than A-366833 at hα4β2 (EC_{50} = 0.05 μM, 133% vs. nicotine) with even greater activity at the α3β4 subtype (EC_{50} = 0.01 μM, 103% vs. nicotine). Among the stereoisomers **3–6**, A-365193 (**4**) and A-424600 (**5**) were approximately 2-fold less potent than A-366833 at the α4β2 nAChR subtype, although the **5** is a full agonist. Neither **4** nor **5** showed any subtype selectivity, however, as they activated α3β4 nAChRs with EC_{50} values of 13.7 μM (max. response 47%) and 7.1 μM (max. response 84%), respectively. Finally, A-369452 (**6**) exhibited nearly 10-fold higher potency (EC_{50} = 0.6 μM, max. response 123%) than A-366833 at the recombinant human α4β2 nAChR subtype, and even greater activity (EC_{50} = 0.3 μM, max. response 102%) at the recombinant human α3β4 nAChR subtype. Thus, among analogs within this group, only A-366833 achieved substantial α4β2 nAChR subtype selectivity (Table 1).

In order to assess the potential for off-target activity of A-366833, it was evaluated by radioligand binding against a panel of 75 receptors, channels and enzyme targets (Cerep). Up to a concentration of 10 μM, A-366833 showed no significant inhibition (>70%) of radioligand binding except at the $5HT_3$ receptor (85%).

3.2. *In vivo efficacy*

3.2.1. *Mice abdominal constriction*

Injection of 0.6% acetic acid into the peritoneal cavity of mice evoked abdominal constriction responses characterized by abdominal stretching combined with an exaggerated extension of the hind limbs. Systemic administration of A-366833 decreased acetic acid induced abdominal constrictions in a dose-related manner (Fig. 2). While no reductions in the number of abdominal constrictions were noted at a dose of 0.019 μmol/kg (i.p.), doses of 0.062 μmol/kg (i.p) and 0.19-μmol/kg (i.p.) of A-366833 reduced constrictions by 38% and 77%, respectively. At the highest dose tested (i.p. 0.62 μmol/kg), animals exhibited 85% diminution of abdominal constrictions. (As a positive control, epibatidine was fully efficacious in this model at 0.012 μmol/kg.)

3.2.2. *Rat acute thermal pain*

Intraperitoneal administration of A-366833 increased paw withdrawal latencies in the rat acute thermal pain model (Fig. 3). Doses of 0.62 μmol/kg and 1.9 μmol/kg showed no antinociceptive effects relative to control animals whereas significant antinociceptive effects of A-366833 were observed at higher doses (6.2–19 μmol/kg). By comparison, epibatidine is much more potent in this model (ED_{50} value of 0.004 μmol/kg, Curzon et al. [38]). In contrast to epibatidine, however no apparent behavioral side effects, such as hypoactivity, ataxia,

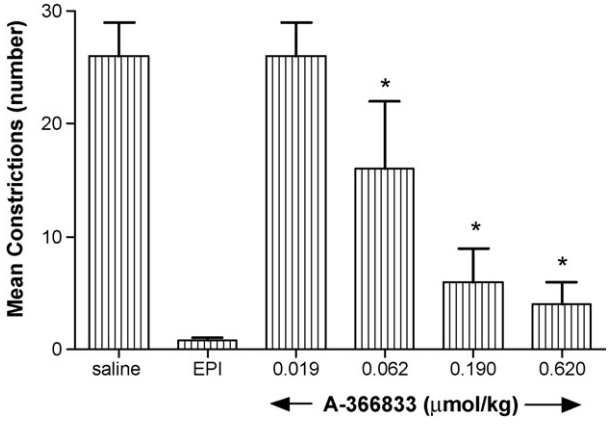

Fig. 2 – Antinociceptive effects of A-366833 in the acetic acid-induced abdominal constriction model in mouse. Results are presented as number of constrictions during the test period (mean ± S.E.M.), *n* = 6/group, (*) Indicates significant (*P* < 0.05) differences vs. saline treated group.

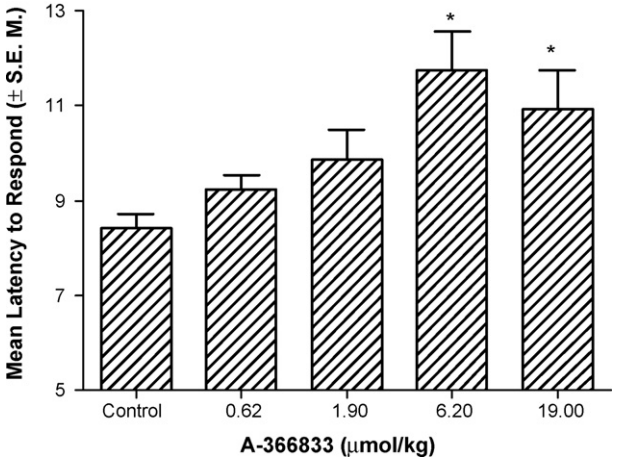

Fig. 3 – Antinociceptive effects of A-366833 in the rat acute thermal pain assay (hot box). A-366833 produced a significant dose-dependent antinociceptive effect after systemic (i.p.) administration. Values represent the mean latency to paw withdrawal (±S.E.M.); n = 6–9/group. (*) Significantly ($P < 0.05$) different from saline treated rats.

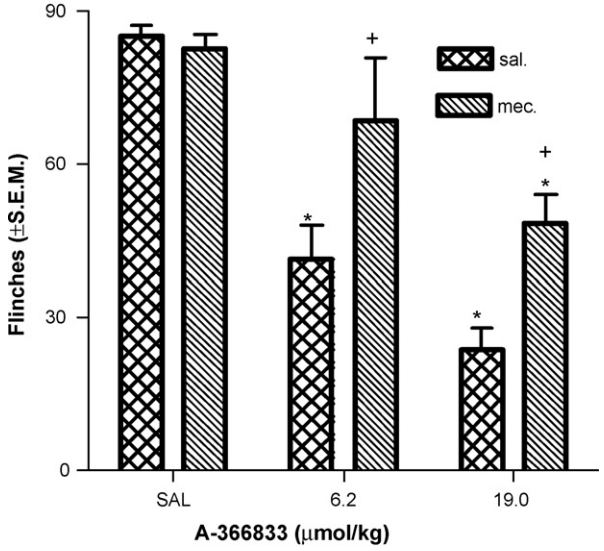

Fig. 5 – Effect of mecamylamine pretreatment on the analgesic effect of A-366833 in phase 2 of rat formalin test. Mecamylamine HCl (5.0 μmol/kg) was administrated 10 min prior to the injection of A-366833 (n = 6/group). (*) Indicates significantly ($P < 0.05$) different from saline/saline group. (+) Indicates significantly ($P < 0.05$) different from saline/A-366833 group.

sedation and respiratory changes [17,18], were observed at efficacious doses of A-368833.

3.2.3. *Formalin model*

Next, the effect of systemic A-366833 treatment on phase 2 responses of the formalin model was investigated. A-366833 evoked dose-dependent reductions in the nocifensive responses after formalin injection to the hind paw (1.9–19.0 μmol/kg, i.p. Fig. 4). Control animals evoked mean flinches of 80 ± 1.8 during the 20-min time-period measured 30–50 min. after the injection of formalin into the rear paw. At a dose of 1.9 μmol/kg (i.p.), A-366833 significantly attenuated nocifensive responses, decreasing flinches by about 50%. At 19 μmol/kg (i.p.), A-366833 demonstrated the most robust analgesic effect (mean flinches, 19 0 ± 4.3).

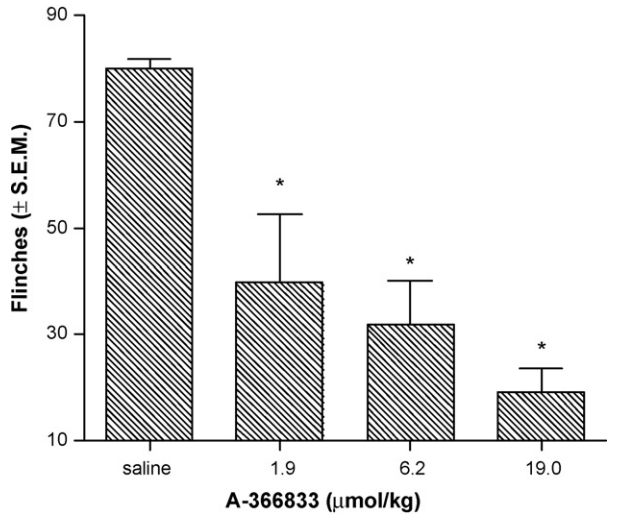

Fig. 4 – Effect of A-366833 in the formalin model of persistent pain. Administration of A-366833 after the injection of formalin produced significant dose-dependent analgesic effects during phase 2 of the formalin test (n = 5/group). Values represent number of flinches. (*) Indicates significantly ($P < 0.05$) different from saline treated rats.

To establish the mechanism by which A-366833 produced analgesic effects in the formalin model, the effect of pretreatment with the non-competitive nAChR channel blocker mecamylamine was examined. Mecamylamine (5.0 μmol/kg, i.p.) was injected 10 min before the administration of saline or A-366833. Mecamylamine alone had no effect on the number of flinches in phase 2 of the formalin test. However, as shown in Fig. 5, the analgesic effect of A-366833 at the dose of 6.2 μmol/kg (i.p.) was blocked by pretreatment with the nAChR antagonist mecamylamine (5.0 μmol/kg). The effect of a higher dose of A-366833 (19 μmol/kg, i.p.) was significantly attenuated by pretreatment with mecamylamine indicating that the analgesic effects of A-366833 in rat formalin model are mediated by agonist activity at nAChRs. Furthermore, this result argues against significant contribution of α9α10 nAChRs in the effects of A-366833, since α9α10 analgesia is evoked by antagonists [23].

3.2.4. *Spinal nerve ligation model*

A-366833 (1.9–19 μmol/kg, i.p.) also induced significant dose-dependent reversal of mechanical allodynia in rats with neuropathy secondary to the tight ligation of spinal nerves L5 and L6 (Fig. 6). At the 15-min time point following injection of A-366833 (19 μmol/kg, i.p.), maximal anti-allodynic responses averaging 13.90 ± 0.70 (g) were observed. The anti-allodynic was maintained, although at reduced levels through the 30-

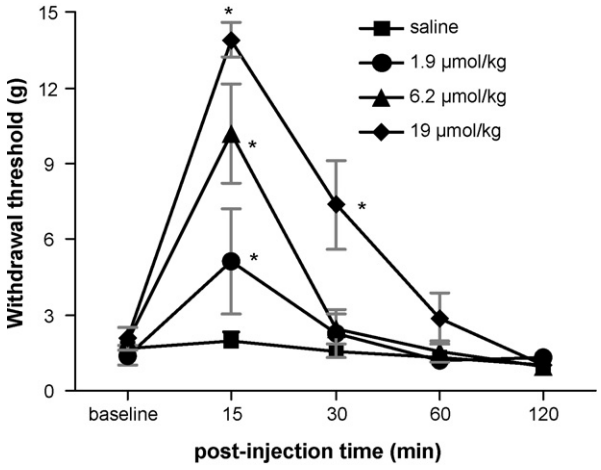

Fig. 6 – Effects of multiple doses of A-366833 on paw withdrawal threshold (mean ± S.E.M.) in a test of mechanical allodynia in the rat spinal nerve ligation (SNL) model of neuropathic pain. Paw withdrawal threshold (gram force) was determined using von Frey filament stimulation and the Dixon's up-down method. Measures were taken before agonist injection (baseline) and at 15, 30, 60 and 120 min after agonist injection. Six rats were used at each dose. (*) Significant ($P < 0.05$) differences vs. saline treated rats at the corresponding time intervals ($n = 6$/group).

min time point at the same dose. By the 60-min time point, the antiallodynic effect of A-366833 had abated. This dose (19 μmol/kg, i.p.) was well tolerated, and behavioral side effects, such as prostration and ataxia, typically seen with non-selective nicotinic agonists, were not observed following treatment with A-366333. Antiallodynic efficacy was also noted at lower doses (1.9–6.2 μmol/kg, i.p.), although these effects were limited in duration to the 15-min time point, with no significant analgesia by 30 post-dose.

In this model, pretreatment with the nAChR antagonist mecamylamine (5.0 μmol/kg, i.p., 10 min prior to the injection of A-366833) completely blocked the anti-allodynic effects of A-366833 (19 μmol/kg, i.p.) (Fig. 7), confirming that the effects are nAChR agonist mediated.

3.3. *Brain penetration and pharmacokinetic properties in the rat*

It has been previously shown that the central activity of nAChR agonists is important for their broad-spectrum analgesic effects [5–8]. The ability of A-366833 to enter the brain was assessed by measuring concentrations of A-366833 in brain and blood plasma in rat. A-366833 rapidly distributed into the brain after the i.p. administration (6.2 μmol/kg) with a brain: plasma ratio of 1–2:1, indicating efficient CNS penetration. Since *in vivo* studies were conducted by i.p. administration, the pharmacokinetic properties of A-366833 were assessed after i.p. dosing in rats. Plasma concentrations of A-366833 following a 3.0 μmol/kg (i.p.) in rats reached C_{max} of 108 ng/mL with a mean T_{max} of 0.3 h ($n = 3$). In addition, the pharmacokinetic profile was also assessed after i.v. and p.o. administration of 6.2 μmol/kg dose in rats ($n = 3$). A-366833 showed plasma clearance (CLp), volumes of distribution (V_β) and half-life values of 3.02 L/h/kg, 6.6 L/h and 1.5 h, respectively. A-366833 also showed excellent oral bioavailability (73%). Since emetic liability was routinely tested in ferrets, the pharmacokinetic profile of A-366833 was assessed in this species as well. Plasma concentrations of A-366833 following a 2.5 μmol/kg dose (i.p.) in ferret showed a mean C_{max} of 373 ng/mL with a mean T_{max} of 0.25 h ($n = 3$) and a half life of 1.5 h.

3.4. *Emesis profile in ferrets*

Nausea and emesis have been identified as dose-limiting adverse effects for multiple experimental nAChR ligands [9–13,39]. We have previously described a ferret emesis model to evaluate the emetic potential of these compounds [31,32]. Administration of 10 μmol/kg A-366833 (i.p.) did not produce emesis in ferrets ($n = 6$). Emesis, however, was observed at higher doses. We compared the highest dose to produce no emesis (the "no-emesis threshold") in ferret to exposures corresponding to the minimal efficacious dose (MED) in rodent pain models to determine a preclinical therapeutic index for A-366833. This can be done by comparing the relevant doses (Table 2), providing therapeutic indices of 1.6–5.3, depending on the model. Since, however, the pharmacokinetics differs between rat and ferret, the therapeutic index was also calculated using plasma exposures (based upon C_{max} extrapolated from PK experiments described in the previous section). Specifically, since plasma exposures for a given dose of A-366833 were higher in ferret compared to rat, this analysis provides higher therapeutic indices. Thus, the peak plasma exposure in ferret at 10 μmol/kg (i.p.) projects to 1492 ng/mL. Conse-

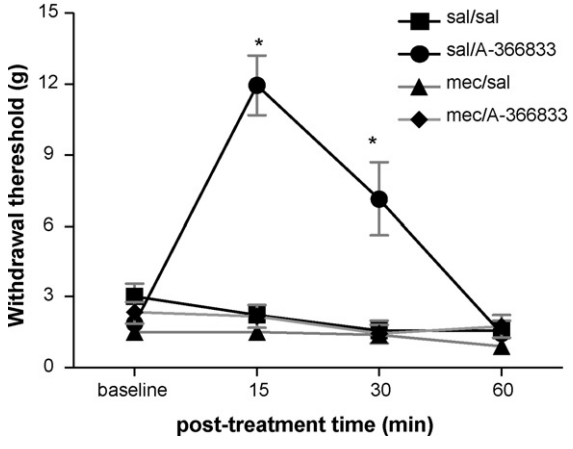

Fig. 7 – Effect of mecamylamine pretreatment on the anti-allodynic effect of 19 μmol/kg A-366833 (i.p.) in SNL neuropathic pain model. Mecamylamine HCl (5 μmol/kg, i.p.) was administered 10 min before A-366833. Withdrawal thresholds to a mechanical stimulus were determined prior to mecamylamine administration and 15, 30 and 60 min post A-366833 administration. (*) Significant ($P < 0.05$) differences vs. other treatment groups at the corresponding time intervals ($n = 6$/group).

Table 2 – Therapeutic Index of A-366833

Model	Minimal efficacious dose (MED) (μmol/kg)	Peak plasma concentration (PPC) (ng/mL)	Therapeutic index	
			MED[a]	PPC[b]
Hot-box	6.2	223	1.6	6.7
Formalin	1.9	68	5.3	21.9
SNL	1.9	68	5.3	21.9

[a] Therapeutic index was calculated by dividing no emesis threshold dose in ferret (10 μmol/kg) by corresponding minimal efficacious dose in the respective pain model assessed in the rat.
[b] Therapeutic index was calculated by dividing the peak plasma concentrations (1492 ng/mL, no emesis threshold dose in ferret) by C_{max} level corresponding to the minimal efficacious dose in the respective pain model assessed in the rat.

quently, the therapeutic index was calculated by dividing the peak plasma concentrations (1492 ng/mL, no emesis threshold dose in ferret) by the peak plasma levels corresponding to the minimal efficacious dose in the respective pain models assessed in the rat. As shown in Table 2, A-366833 produced a favorable therapeutic index vs. no emesis threshold of 6.7, 21.9 and 21.9 in models of acute thermal pain, formalin and SNL, respectively.

3.5. *Discussion and summary*

Nicotine and other nAChR agonists, such as epibatidine, have previously demonstrated analgesic activity in a wide variety of preclinical pain models [5–8]. For example, although the mild analgesic effect of nicotine (**1**) in a cat model of visceral pain was reported decades ago [40], its limited efficacy of nicotine in eliciting analgesia, as well as accompanying adverse side effects (convulsions, hypothermia, loss of motor coordination, hypothermia and emesis) precludes its clinical use as an analgesic agent [41–45]. Epibatidine was reported to evoke a robust analgesic response superior to morphine, but at efficacious doses, this compound exhibited severe adverse side effects and toxicity [46–48], indicating lack of therapeutic index between analgesia and nAChR-mediated side effects. Although therapeutic indices of newer agents including ABT-594 are somewhat improved relative to epibatidine [4], opportunities exist to further separate the analgesic activity from side effects.

Although A-366833 exhibited relatively lower α4β2 binding affinity compared to compounds like epibatidine and ABT-594, its binding affinity (K_i = 3 nM) is comparable to that of nicotine (K_i = 1 nM). Compared to the non-selective nAChR agonist epibatidine, A-366833 showed approximately 60-fold weaker binding affinity and 110-fold weaker functional potency for activation of the α4β2 nAChR subtype. Interestingly, A-366833 exhibited superior selectivity towards the α4β2 nAChR subtype compared to activation of α3β4 nAChR subtype. Since A-366833 demonstrated improved α4β2 vs. α3β4 nAChR subtype selectivity, the compound was profiled in a variety of rodent pain models indicating multiple pain states, such as models of writhing pain (mice ACA), acute nociceptive pain (rat acute thermal pain), persistent nociceptive pain (rat formalin) and neuropathic pain (rat SNL). A-366833 exhibited significant analgesic effects in a variety of rodent pain models. For example, A-366833 exhibited excellent potency (0.062–0.62 μmol/kg) and robust efficacy in mouse abdominal construction assay, model of visceral pain. In three other models in rat – hot box for acute thermal pain, formalin model of persistent pain and spinal ligation model for neuropathic pain, A-366833 was very efficacious at doses in the range of 1.9–6.2 μmol/kg.

Pretreatment with mecamylamine (5.0 μmol/kg) significantly attenuated the analgesic effect of A-366833 assessed in the phase 2 of the formalin model and completely blocked the anti-allodynic effects evoked by A-366833 (19 μmol/kg, i.p.) in the SNL model. These observations suggest that the analgesic effects of A-366833 in models of persistent nociceptive and neuropathic pain are nAChR mediated. As noted in the Introduction, it has recently been shown that antagonism of peripherally disposed α9α10 nAChRs also leads to an analgesic response, and is especially effective in models of neuropathic pain [22,23]. It is not trivial to positively define the analgesic mechanism for a nAChR ligand, in part because relatively few nAChR ligands have been evaluated for activity at α9α10. Moreover, some agonists at the α4β2 nAChR, including nicotine, act as antagonists of the α9α10 receptor [24]. The Abbott compounds described herein have not been evaluated for activity at the α9α10 nAChR, and contribution of this receptor to the analgesic activity cannot be ruled out entirely. Nevertheless, the observation that analgesic responses are blocked by the (non-competitive) nAChR antagonist mecamylamine is more consistent with those effects arising from agonist activation of α4β2 nAChRs.

Since improved tolerability of nAChR agents remains a major goal in the development of nAChR-based therapeutics, side effect profiles such as emesis [9–13,39], were evaluated to determine therapeutic margins. As demonstrated in Table 2, A-366833 showed substantial separation of analgesic vs. emetic effects. Although emesis was observed at higher doses, the favorable therapeutic index of A-366833 supports a profile adequate for clinical advancement. The separation of analgesic effects from gastrointestinal tolerability demonstrates that agonists with improved α4β2 (vs. α3β4) agonist selectivity can achieve broad-spectrum efficacy in a variety of animal pain models, without concurrent adverse effects.

Acknowledgements

The authors would like to thank Drs. Murali Gopalakrishnan and Lance Lee for assistance with the preparation of this manuscript.

REFERENCES

[1] Kennedy JD. Neuropathic pain: molecular complexity underlies continuing unmet medical need. J Med Chem 2007;50:2547–56.
[2] Jensen AA, Frolund B, Liljefors T, Krogsgaard-Larsen P. Neuronal nicotinic acetylcholine receptors: structure revelations, targets identifications, and therapeutic inspirations. J Med Chem 2005;48:4705–45.
[3] Bunnelle WH, Dart MJ, Schrimpf MR. Design of ligands for the nicotinic acetylcholine receptors: the quest for selectivity. Curr Med Chem 2004;4:299–334.
[4] Decker MW, Rueter LR, Bitner RC. Nicotinic acetylcholine receptor agonists: a potential new class of analgesics. Curr Top Med Chem 2004;4:369–84.
[5] Decker M. Neuronal nicotinic acetylcholine receptors as a target for the treatment of neuropathic pain. Drug Dev Res 2006;67:355–9.
[6] Rueter LE, Donnelly-Roberts DL, Curzon P, Briggs CA, Anderson DJ, Bitner RS. A-85380: a pharmacological probe for the preclinical and clinical investigation of the α4β2 neuronal nicotinic acetylcholine receptor. CNS Drug Rev 2006;12:100–12.
[7] Damaj MI, Wiley JL, Martin BR, Papke RL. In vivo characterization of a novel inhibitor of CNS nicotinic receptors. Eur J Pharmol 2005;521:43–8.
[8] Bannon AW, Decker MW, Holladay MW, Curzon P, Donnelly–Roberts D, Puttfarcken PS, et al. Broad spectrum, non-opioid analgesic activity by selective modulation of neuronal nicotinic acetylcholine receptors. Science 1998;279:77–81.
[9] Andrews PLR, Friedman AI, Liu Y, Smith JE, Sims DW. Potential energetic implications of emesis in the house musk shrew (*Suncus murinus*). Physiol Behav 2005;84:519–24.
[10] Rudd JA, Wai MK. Genital grooming and emesis induced by vanilloids in *Suncus murinus*, the house musk shrew. Eur J Pharmcol 2001;422:185–95.
[11] Boyce S, Webb JK, Shepheard SL, Russell MGN, Rupniak NMJ. Anagesic and toxic effects of ABT-594 resemble epibatidine and nicotine in rats. Pain 2000;85:443–50.
[12] Beleslin DB, Krstic SK. Further studies on nicotine-induced emesis: nicotinic mediation in area postrema. Physiol Behav 1987;39:681–6.
[13] Spealman RD. Maintenance of behavior by postponement of scheduled injections of nicotine in squirrel monkeys. J Pharmcol Exp Ther 1983;227:154–9.
[14] Sullivan JP, Bannon AW. Epibatidine: pharmacological properties of a novel nicotinic acetylchloine receptor agonist and analgesic agent. CNS Drug Rev 1996;2:21–39.
[15] Millar NS. Assembly and subunit diversity of nicotinic acetylcholine receptors. Biochem Soc Trans 2003;31:869–74.
[16] Khan IM, Stanislaus S, Zhang L, Taylor P, Yaksh TL. A-85380 and epibatidine each interact with disparate spinal nicotinic receptor subtypes to achieve analgesia and nociception. J Pharmacol Exp Ther 2001;297:230–9.
[17] Cucchiaro G, Chaijale N, Commons KG. The dorsal raphe nucleus as a site of action of the antinociceptive and behaviral effects of the α4 nicotinic receptor agonist epibatidine. J Pharmacol Exp Ther 2005;313:389–94.
[18] Rueter LE, Kohlhaas KL, Curzon P, Surowy CS, Meyer MD. Peripheral and central sites of action for A-85380 in the spinal nerve ligation model of neuropathic pain. Pain 2003;103:269–76.
[19] Bitner RS, Nikkel AL, Curzon P, Donnelly-Roberts DL, Puttfarcken PS, Namovic M, et al. Reduced nicotinic receptor-mediated antinociception following in vivo antisense knock-down in rat. Brain Res 2000;871:66–74.
[20] Marubio LM, del Mar Arroyo-Jimenez M, Cordero-Erausquin M, Lena C, Le Novere N, de Kerchove d'Exaerde A, et al. Reduced antinociception in mice lacking neuronal nicotinic receptor subunits. Nature 1999;398:805–10.
[21] Picciotto MR, Zoli M, Rimondini R, Lena C, Marubio LM, Pich EM, et al. Acetylcholine receptors containing the β2 subunit are involved in the reinforcing properties of nicotine. Nature 1998;391:173–7.
[22] Vincler M, McIntosh JM. Targeting the α9α10 nicotinic acetylcholine receptor to treat severe pain. Expert Opin Ther Targets 2007;11:891–7.
[23] Vincler M, Wittenauer S, Parker R, Ellison M, Olivera BM, McIntosh JM. Molecular mechanism for analgesia involving specific antagonism of α9α10 nicotinic acetylcholine receptors. Proc Natl Acad Sci USA 2006;103:17880–4.
[24] Gomez-Casati ME, Fuchs PA, Elgoyhen AB, Katz E. Biophysical and pharmacological characterization of nicotinic cholinergic receptors in rat cochlear inner hair cells. J Physiol 2005;566:103–18.
[25] Ji J, Schrimpf MR, Sippy KB, Bunnelle WH, Li T, Anderson DJ, et al. Synthesis and structure–activity relationship (SAR) studies of 3,6-diazabicyclo[3.2.0]-heptanes as novel α4β2 nicotinic acetylcholine receptor (nAChR) selective agonists. J Med Chem 2007;50:in press.
[26] Pabreza LA, Dhawan S, Kellar KJ. [^{3}H]-Cytisine binding to nicotinic cholinergic receptors in brain. Mol Pharmacol 1991;39:9–12.
[27] Honore P, Mikusa J, Bianchi B, McDonald H, Cartmell J, Faltynek C, et al. TNP-ATP, a potent P_2X_3 receptor antagonist, blocks acetic acid-induced abdominal constriction in mice: comparison with reference analgesics. Pain 2002;96:99–105.
[28] Bannon AW, Decker MW, Curzon P, Buckley MJ, Kim DJ, Radek RJ, et al. ABT-594 [(*R*)-5-(2-azetidinylmethoxy)-2-chloropyridine]: a novel, orally effective antinociceptive agent acting via neuronal nicotinic acetylcholine receptors. II. In vivo characterization. J Pharmacol Exp Ther 1998;285:787–94.
[29] Damaj MI, Glassco W, Aceto MD, Martin BR. Antinocieptive responses of metanicotine, a selective nicotinic agonist. J Pharmacol Exp Ther 1999;291:390–8.
[30] Kim SH, Chung JM. An experimental model for peripheral neuropathy produced by segmental spinal nerve ligation in the rat. Pain 1992;50:355–63.
[31] Osinski MA, Uchic ME, Seifert T, Shaughnessy TK, Miller LN, Nakane M, et al. Dopamine D2, but not D4, receptor agonists are emetogenic in ferrets. Pharmacol Biochem Behavior 2005;81:211–9.
[32] Osinski MA, Seifert TR, Shaughnessy TK, Gintant GA, Cox BF. Emetic libility testing in ferrets. In: Enna SJ, William M, Ferkany JW, Kenakin T, Porsolt RD, Sullivan JP, editors. Current protocols in pharmacology. New York: John Wiley Sons; 2003. p. 5.31.1–8.
[33] Houghtling RA, Dávila-Carcía MI, Kellar KJ. Characterization of (±)-[^{3}H]epibatidine binding to nicotinic cholinergic receptors in rat and human brain. Mol Pharmacol 1995;48:280–7.
[34] Flores CM, Rogers SW, Pabreza LA, Wolfe BB, Kellar KJ. A subtype of nicotinic cholinergic receptor in rat brain is composed of α4 and β2 subunits and is up-regulated by chronic nicotine treatment. Mol Pharmacol 1992;41:31–7.
[35] Anderson DJ, Williams M, Arneric SP, Pauly JR, Rotert GA, Raszkiewicz JL, et al. Characterization of [3H]-ABT-418: a novel cholinergic channel ligand. J Pharmacol Exp Ther 1995;273:1434–41.
[36] Fitch RW, Xiao Y, Kellar KJ, Daly JW. Membrane potential fluorescence: a rapid and highly sensitive assay for nicotinic receptor channel function. Proc Natl Acad Sci USA 2003;100:4909–14.

[37] Kuntzweiler TA, Arneric SP, Donnelly-Roberts DL. Rapid assessment of ligand actions with nicotinic acetylcholine receptors using calcium dynamics and FLIPR. Drug Dev Res 1998;44:14–20.
[38] Curzon P, Nikkel AL, Bannon AW, Arneric SP, Decker MW. Differences between the antinociceptive effects of the cholinergic channel activators A-85380 and (±)-epibatidine in rats. J Pharmacol Exp Ther 1998;287:847–53.
[39] Sullivan JP. Neuroscience and pain. http://media.corporateir.net/media_files/nys/abt/rdday/NeuroPain.pdf.
[40] Davis L, Pollock LJ, Stone TT. Visceral pain. Surg Gynecol Obstet 1932;55:418–26.
[41] Campbell VC, Taylor RE, Tizabi Y. Antinociceptive effects of alcohol and nicotine: involvement of the opioid system. Brain Res 2006;1097:71–7.
[42] Cepeda-Benito A, Reynoso JT, Davis KW, Susabda A, Mendez IA, Harraid JH. Interdose interval effects on the development of contextual tolerance to nicotine's analgesic effects in rats (*Rattus norvegicus*). Exp Clin Psychopharm 2006;14:180–9.
[43] Cepeda-Benito A, Davis KW, Reynoso JT, Harraid JH. Associative and behavioral tolerance to the analgesic effects of nicotine in rats: tail-flick and paw-lick assays. Psychopharmacology 2005;180:224–33.
[44] Glennon RA. Nicotine and pain. Med Chem Res 2004;13:74–7.
[45] Tripathi HL, Martin BR, Aceto MD. Nicotine-induced antinociception in rats and mice: correlation with nicotine brain levels. J Pharmacol Exp Ther 1982;221:91–6.
[46] Daly JW, Garraffo HM, Spande TF, Decker MW, Sullivan JP, Williams M. Alkaloids from frog skin: the discovery of epibatidine and the potential for developing novel non-opoid analgesics. Nat Prod Rep 2000;17:131–5.
[47] Badio B, Garraffo HM, Spande TF, Daly JW. Epibatidine: discovery and definition as a potent analgesic and nicotinic agonist. Med Chem Res 1994;4:440–8.
[48] Badio B, Daly JW. Epibatidines: a potent analgesic and nicotinic agonist. Mol Pharmacol 1994;45:563–9.